High-power terahertz optical pulse generation with a dual-wavelength harmonically mode-locked Yb:YAG laser

2013 Laser Phys. 23 075803

(http://iopscience.iop.org/1555-6611/23/7/075803)

IOP PUBLISHING LASER PHYSICS
Laser Phys. **23** (2013) 075803 (5pp) doi:10.1088/1054-660X/23/7/075803

High-power terahertz optical pulse generation with a dual-wavelength harmonically mode-locked Yb:YAG laser

W Z Zhuang, M T Chang, K W Su, K F Huang and Y F Chen[1]

Department of Electrophysics, National Chiao Tung University, Hsinchu, 30010, Taiwan

E-mail: yfchen@cc.nctu.edu.tw

Received 31 January 2013
Accepted for publication 8 April 2013
Published 10 June 2013
Online at stacks.iop.org/LP/23/075803

Abstract
We report on high-power terahertz optical pulse generation with a dual-wavelength harmonically mode-locked Yb:YAG laser. A semiconductor saturable absorber mirror is developed to achieve synchronously mode-locked operation at two spectral bands centered at 1031.67 and 1049.42 nm with a pulse duration of 1.54 ps and a pulse repetition rate of 80.3 GHz. With a diamond heat spreader to improve the heat removal efficiency, the average output power can be up to 1.1 W at an absorbed pump power of 5.18 W. The autocorrelation traces reveal that the mode-locked pulse is modulated with a beat frequency of 4.92 THz and displays a modulation depth to be greater than 80%.

(Some figures may appear in colour only in the online journal)

1. Introduction

Ultrashort pulse lasers with terahertz (THz) beat frequencies have become more and more important in a wide range of applications, such as medical imaging [1], plasma physics [2], quantum communication [3], optical sampling [4], and astrophysics [5]. Dual-wavelength synchronously mode-locked lasers [6–8] have been extensively used to generate the ultrashort optical pulse trains with THz beat frequencies. Demonstrations of dual-wavelength synchronous mode locking include Ti:sapphire lasers [8–15], semiconductor lasers [6], and rare-earth doped solid state lasers, such as Nd-doped disordered crystal lasers [7, 16–19] and the Yb:LYSO laser [20].

Among rare-earth doped crystals, the Yb:YAG crystal has been identified to be a promising material for generating compact efficient ultrashort laser pulses [21–26], owing mainly to the small quantum defect, broad absorption and fluorescence spectra, and high quantum efficiency. A dual-wavelength mode-locked Yb:YAG ceramic laser at 1033.6 and 1047.6 nm was recently demonstrated in a single cavity [25]. However, since the optical paths of the dual-wavelength modes were spatially separate in the laser cavity, there was no observation of an ultrashort pulse train with a THz beat frequency. Besides, the low optical-to-optical conversion efficiency leads to the average output power being only 8 mW. Therefore, it is highly desirable and practically useful to develop a high-power dual-wavelength synchronously mode-locked Yb:YAG laser to generate ultrashort pulses with THz beat frequencies.

The spontaneous emission spectrum of the Yb:YAG crystal reveals that there are two main peaks under optical excitation at 940 nm [27, 28]: the primary and secondary peaks are located around 1032 nm and 1049 nm, respectively. One of the key issues for achieving dual-wavelength operation in a Yb:YAG laser is to preciously control the gain-to-loss ratios at 1032 and 1049 nm [29]. On the other hand, the synchronization of dual-wavelength mode-locked beams is indispensable for generating an ultrashort pulse train with a THz beat frequency. It has been shown that the cross saturation of a saturable absorber is beneficial to the synchronization of dual-wavelength mode-locked beams [7, 16]. In this work, we design a semiconductor saturable absorber mirror (SESAM)

[1] Address for correspondence: Department of Electrophysics, National Chiao Tung University, 1001 TA Hsueh Road, Hsinchu, 30050, Taiwan.

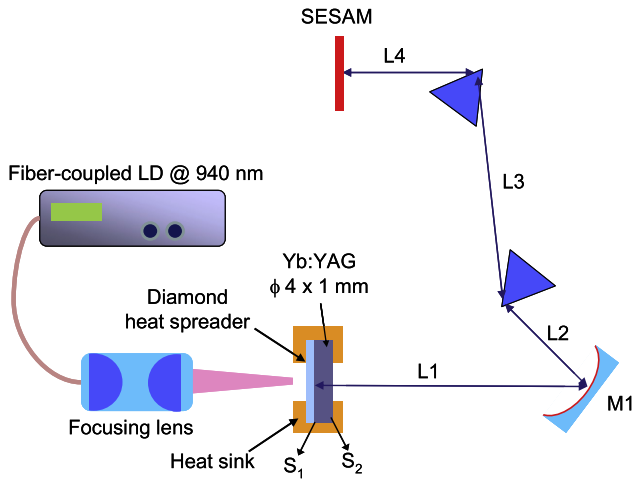

Figure 1. The schematic diagram of the mode-locked Yb:YAG laser experimental setup. (S_1: HT at 940 nm, HR at 1030–1100 nm; S_2: HT at 1030–1100 nm, HR at 940 nm; HT: high transmission; HR: high reflection).

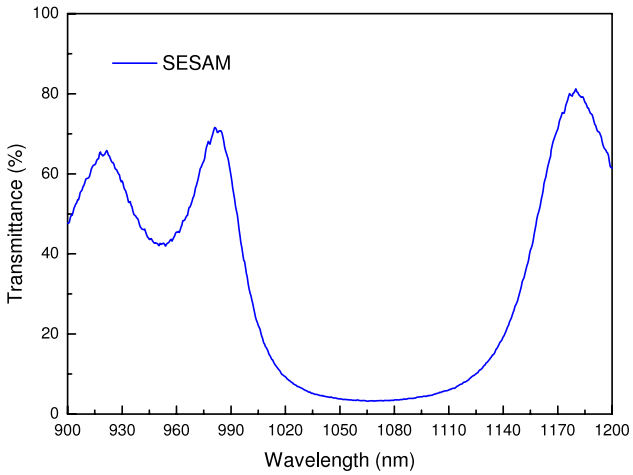

Figure 2. Transmittance spectra of the SESAM.

not only to assist the synchronous mode locking but also to balance the output coupling for achieving dual-wavelength operation at 1032 and 1049 nm. With the fabricated SESAM, we successfully develop a high-power dual-wavelength harmonically mode-locked Yb:YAG laser to generate a pulse train with a pulse duration of 1.54 ps at a repetition rate of 80.3 GHz. A diamond heat spreader is employed to enhance the heat removal efficiency of the Yb:YAG medium for scaling up the output power [23, 26]. The maximum average output power can be up to 1.1 W under an absorbed pump power of 5.18 W, corresponding to an optical-to-optical conversion efficiency of 21.2% and a slope efficiency of 29.4%. The auto-correlation traces display a deep modulation with a period corresponding to a beat frequency of 4.92 THz. Since the overall modulation depth is greater than 80%, the effective pulse duration within the mode-locked pulse is as short as 83 fs.

2. Experimental setup

Figure 1 presents the schematic of the experimental setup. The gain medium was an 11 at.% doped Yb:YAG crystal cut along the [111] direction of 1.03 mm in length and 4 mm in diameter. One end facet of the crystal, coated for high reflection (HR, $R > 99.8\%$) from 1030 to 1100 nm and high transmission (HT, $T > 95\%$) at 940 nm, served as the front mirror. The rear facet was coated for high reflection (HR, $R > 99\%$) at 940 nm to increase the absorption efficiency of the pump power and with high transmission (HT, $T \approx 95\%$) from 1030 to 1100 nm. It has been confirmed [23] that the partial reflection ($R \approx 5\%$) on the rear facet for the lasing spectral range can introduce a significant etalon effect to achieve harmonic mode locking. An uncoated, single crystal synthetic diamond, 4.5 mm square and 0.5 mm in thickness, was used as a heat spreader and capillary bonded to the front mirror side of the gain medium, as described in [23, 26]. The transmittance of the diamond heat spreader was about 70% at 940 nm. The front facet of the diamond was in contact with a copper heat sink which was cooled by a thermal-electric cooler (TEC) and maintained at a temperature of 14 °C. The rear facet of the gain medium was tightly attached to a copper plate with a hole of 2 mm in diameter, where an indium foil was used to improve the thermal contact. The pumping source was a 940-nm fiber-coupled laser diode with a core diameter of 400 μm and a numerical aperture of 0.2. A focusing lens with 25 mm focal length and 90% coupling efficiency was used to re-image the pump beam into the laser crystal. The pump spot radius was approximately 220 μm. A V-shaped cavity was used in the experiment, where L1, L2, and L4 were 275 mm, 244 mm, and 65 mm, respectively. M1 was a concave mirror with a radius of curvature (ROC) of 550 mm and coated for high reflection (HR, $R > 99\%$) from 1030 to 1100 nm. A pair of SF10 prisms with a tip-to-tip distance (L3) of 480 mm was employed to compensate the cavity dispersion. A SESAM was designed to assist the synchronous mode locking and to balance the output coupling for achieving dual-wavelength operation. The modulation depth of the SESAM was found to be approximately 1.2% at 1040 nm. The SESAM device was monolithically grown on an undoped 350 μm thick GaAs substrate by metalorganic chemical vapor deposition (MOCVD) to comprise a single strained $In_{0.27}Ga_{0.73}As$/GaAs quantum well (QW) grown on the Bragg mirror. The QW has a thickness of 8 nm. The Bragg mirror consists of ten pairs of AlAs/GaAs quarter-wavelength layers. Figure 2 shows the transmittance spectrum for the SESAM. It can be seen that the transmittances are approximately 5.8% and 3.8% at 1032 and 1049 nm, respectively. The back side of the GaAs substrate was coated for antireflection at 1040 nm ($R < 1\%$).

3. Experimental results and discussion

Figure 3 depicts the average output power versus the absorbed pump power in dual-wavelength harmonically mode-locked operation. The maximum average output power is approximately 1.1 W under a maximum absorbed pump power of 5.18 W, corresponding to an optical-to-optical conversion efficiency of 21.2% and a slope efficiency

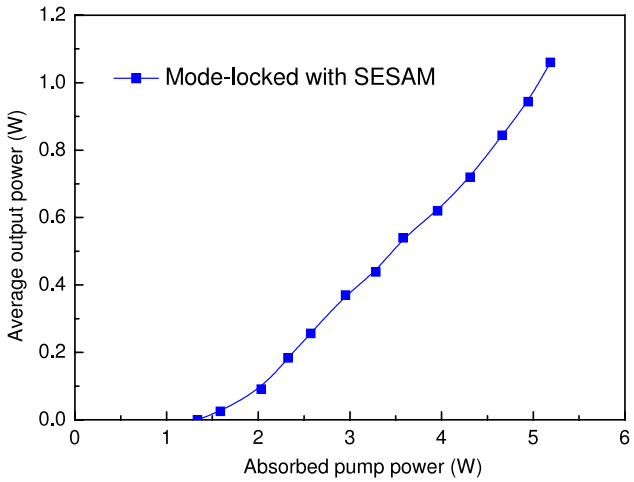

Figure 3. Dependence of the averaged output power on the absorbed pump power in dual-wavelength harmonically mode-locked operation.

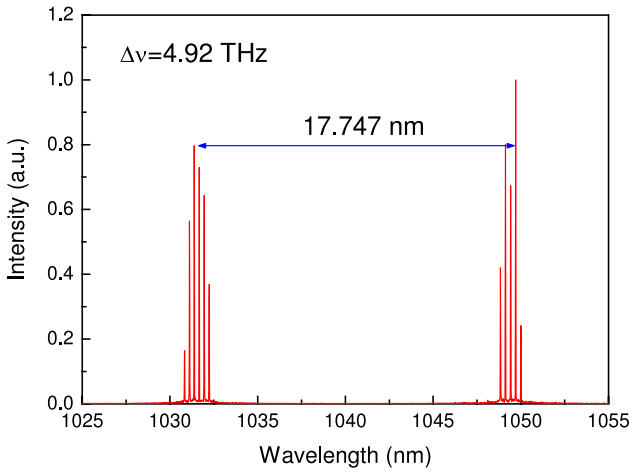

Figure 4. Optical lasing spectrum obtained at the maximum absorbed pump power of 5.18 W.

of 29.4%. The optical-to-optical conversion efficiency is considerably higher than the earlier results of dual-wavelength mode-locked lasers, which range from 0.03% to 10% by utilizing rare-earth doped crystals such as Nd-doped disordered crystals [7, 16–19], Yb:LYSO crystal [20], and Yb:YAG ceramics [25]. With the thermal management of a diamond heat spreader, not only is the output efficiency remarkably increased but also the beam distortion is significantly improved [30].

The optical spectrum of the laser output was measured with a Fourier–Michelson optical interferometer (Advantest, Q8347) with a resolution of 0.003 nm. Figure 4 depicts the experimental result for the lasing spectrum at the maximum absorbed pump power of 5.18 W. It can be seen that there are dual lasing bands with central wavelengths at 1031.67 and 1049.42 nm. As a result, the difference between the central frequencies is 4.92 THz. The values for the full width at half maximum (FWHM) of the spectral bands at 1031.67 nm and 1049.42 nm are 1.08 nm and 0.89 nm, respectively. The spectral intensity ratio of the two bands was numerically calculated to be 1:0.8. The values of the mode spacing within each spectral band are found to be approximately 80.3 GHz. This mode spacing precisely corresponds to the free spectral range of the etalon effect caused by the Yb:YAG crystal with an optical length of about 1.87 mm. It has been demonstrated [23] that partial reflection on the surface of the gain medium could introduce a significant mode selection for effectively generating high-order harmonic mode locking.

The temporal behavior of the laser output was analyzed by exploiting the schemes of first- and second-order autocorrelations. The first-order autocorrelation trace was measured with a Michelson interferometer. The second-order autocorrelation trace was performed with a commercial autocorrelator (APE GmbH, PulseCheck). First of all, we measured the autocorrelation traces in a delay-time span of 50 ps to display the pulse repetition rate of the experimental mode-locked pulse train. For this time span, the resolutions of the first- and second-order autocorrelations are 67 fs and 200 fs, respectively. Figures 5(a) and (b) show the measured results at the maximum absorbed pump power. It can be seen that the laser output exhibits a state of tenth-order harmonic mode locking (relative to the fundamental mode locking pulse repetition rate of 80.3 MHz) with a pulse repetition rate of 80.3 GHz. The tenth-order harmonic mode locking originates from the etalon effect, which is caused by the partial reflection on the surface of the gain medium. The traces of the first- and second-order autocorrelation traces reveal the same pulse period. The similarity indicates that the phase of the optical spectrum is nearly constant [23, 31]. Note that the sampling resolutions shown in figures 5(a) and (b) are not high enough to display the temporal behavior of the THz beat frequency.

To identify the modulation of the beat frequency, we measured the autocorrelation traces with higher resolutions in a delay-time span of 8 ps. For this time span, the resolutions of the first- and second-order autocorrelations are 8 fs and 20 fs, respectively. Figures 6(a) and (b) show the measured results at the maximum absorbed pump power. It can be seen that both the first- and second-order autocorrelations display interference patterns with modulation depths higher than 80% in the mode-locked pulse. Assuming the temporal intensity of the second-order autocorrelation trace to be a sech^2 profile, the duration of the mode-locked pulse can be deduced to be 1.54 ps, as shown in figure 6(b). The periodic modulation within the autocorrelation traces clearly corresponds to the 4.92-THz beat frequency of the dual-wavelength laser. The deep modulation in autocorrelation traces indicates that the dual-wavelength mode-locked pulses are synchronous to a certain extent. Figure 7 shows the second-order autocorrelation trace in a delay-time span of 180 fs to evaluate the pulse duration arising from the beating. In terms of a cosine-like shape, the effective pulse duration of the beating corresponds exactly to the FWHM of the measured autocorrelation trace. As a consequence, the effective pulse duration of the dual-wavelength mode-locked laser is approximately 83 fs.

4. Conclusions

We have experimentally demonstrated a high-power harmonically mode-locked Yb:YAG laser with a pulse duration of

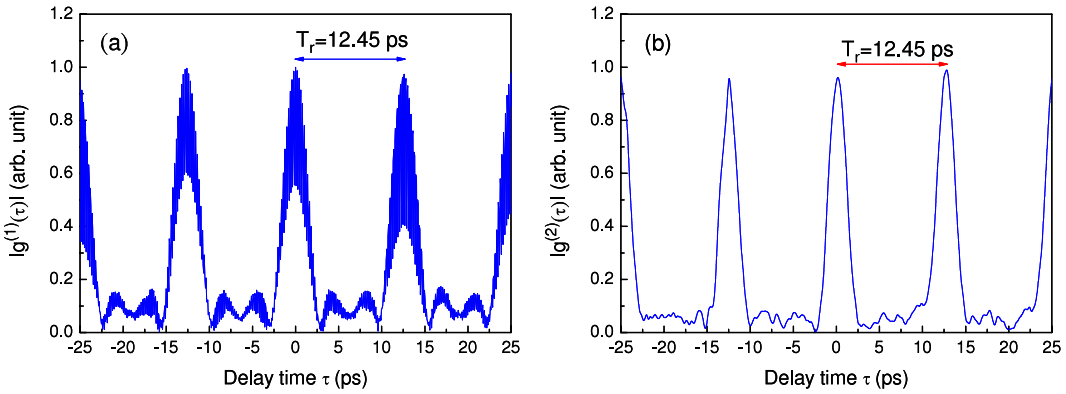

Figure 5. Experimental traces of the temporal behavior of (a) first- and (b) second-order autocorrelations in a delay-time span of 50 ps. Resolution: 67 fs and 200 fs for the first- and second-order autocorrelations, respectively.

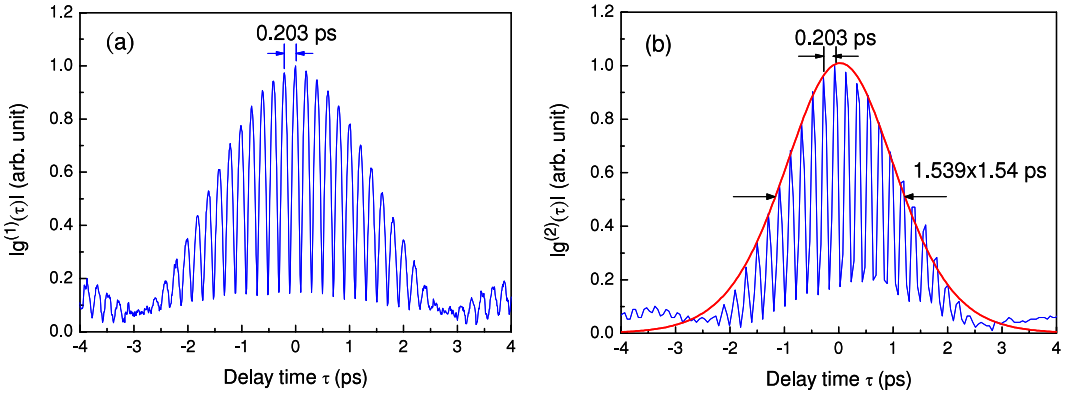

Figure 6. Experimental traces of the temporal behavior of (a) first- and (b) second-order autocorrelations in a delay-time span of 8 ps. Resolution: 8 fs and 20 fs for the first- and second-order autocorrelations, respectively.

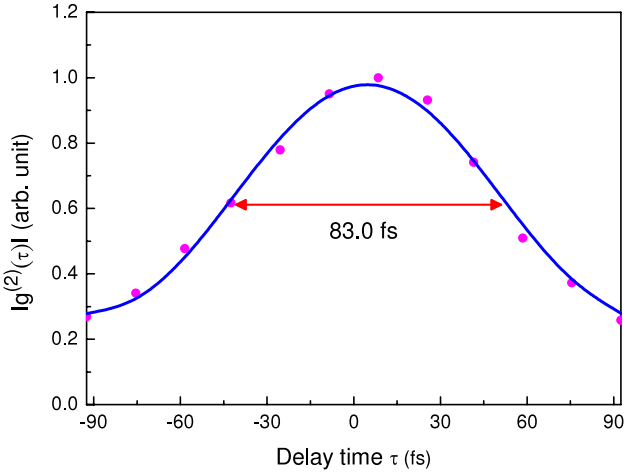

Figure 7. Experimental trace of the temporal behavior of the second-order autocorrelation of the single beat pulse.

1.54 ps at a repetition rate of 80.3 GHz. The power scale-up was improved by employing a diamond heat spreader to enhance the heat removal efficiency of the Yb:YAG crystal. At an absorbed pump power of 5.18 W, the maximum average output power was 1.1 W, corresponding to an optical-to-optical conversion efficiency of 21.2% and a slope efficiency of 29.4%. An appropriate SESAM has been developed to balance the output coupling and to achieve dual-wavelength synchronous mode-locked operation at 1032 and 1049 nm. The autocorrelation traces revealed that the modulation depth of the mode-locked pulse at the beat frequency of 4.92 THz could be generally higher than 80% and the effective pulse duration was as short as 83 fs.

Acknowledgment

The author thanks the National Science Council for their financial support of this research under Contract NSC-100-2628-M-009-001-MY3.

References

[1] Wang T J, Marceau C, Yuan S, Chen Y, Wang Q, Théberge F, Châteauneuf M, Dubois J and Chin S L 2011 *Laser Phys. Lett.* **8** 57–61
[2] Wang T J, Yuan S, Sun Z D, Marceau C, Chen Y, Théberge F, Châteauneuf M, Dubois J and Chin S L 2011 *Laser Phys. Lett.* **8** 295–300
[3] Cole B E, Williams J B, King B T, Sherwin M S and Stanley C R 2001 *Nature* **410** 60–3
[4] Fortier C, Kibler B, Fatome J, Finot C, Pitois S and Millot G 2008 *Laser Phys. Lett.* **5** 817–20
[5] Siegel P H 2007 *IEEE Trans. Antennas Propog.* **55** 2957–65

[6] Pelusi M D, Liu H F, Novak D and Ogawa Y 1997 *Appl. Phys. Lett.* **71** 449–51
[7] Xie G Q, Tang D Y, Luo H, Zhang H J, Yu H H, Wang J Y, Tao X T, Jiang M H and Qian L J 2008 *Opt. Lett.* **33** 1872–4
[8] Zhu C J, He J F and Wang S C 2005 *Opt. Lett.* **30** 561–3
[9] Knox W H and Beisser F A 1992 *Opt. Lett.* **17** 1012–4
[10] Zhang Z and Yagi T 1993 *Opt. Lett.* **18** 2126–8
[11] de Barros M R X and Becker P C 1993 *Opt. Lett.* **18** 631–3
[12] Leitenstorfer A, Fürst C and Laubereau A 1995 *Opt. Lett.* **20** 916–8
[13] Wei Z, Kobayashi Y, Zhang Z and Torizuka K 2001 *Opt. Lett.* **26** 1806–8
[14] Wei Z, Kaboyashi Y and Torizuka K 2002 *Appl. Phys.* B **74** 171–6
[15] Zhu C, Wang Y, He J, Wang S and Hou X 2005 *J. Opt. Soc. Am.* B **22** 1221–7
[16] Xie G Q, Tang D Y, Tan W D, Luo H, Guo S Y, Yu H H and Zhang H J 2009 *Appl. Phys.* B **95** 691–5
[17] Agnesi A, Pirzio F, Reali G, Arcangeli A, Tonelli M, Jia Z and Tao X 2010 *Appl. Phys.* B **99** 135–40
[18] Cong Z H *et al* 2011 *Opt. Express* **19** 3984–9
[19] Xu J L, Guo S Y, He J L, Zhang B Y, Yang Y, Yang H and Liu S D 2012 *Appl. Phys.* B **107** 53–8
[20] Yang Q, Wang Y G, Liu D H, Liu J, Zheng L H, Su L B and Xu J 2012 *Laser Phys. Lett.* **9** 135–40
[21] Uemura S and Torizuka K 2005 *Japan. J. Appl. Phys.* **44** L361–3
[22] Agnesi A, Greborio A, Pirzio F and Reali G 2011 *Opt. Commun.* **284** 4049–51
[23] Chen Y F, Zhuang W Z, Liang H C, Huang G W and Su K W 2013 *Laser Phys. Lett.* **10** 015803
[24] Zhou J Y, Ma J, Dong J, Cheng Y, Ueda K and Kaminskii A A 2011 *Laser Phys. Lett.* **8** 591–7
[25] Yoshioka H, Nakamura S, Ogawa T and Wada S 2010 *Opt. Express* **18** 1479–86
[26] Zhuang W Z, Chen Y-F, Su K W, Huang K F and Chen Y F 2012 *Opt. Express* **20** 22602–8
[27] Weiner A M 2009 *Ultrafast Optics* (New York: Wiley)
[28] Wang X, Xu X, Zhao Z, Jiang B, Xu J, Zhao G, Deng P, Bourdet G and Chanteloup J-C 2007 *Opt. Mater.* **29** 1662–6
[29] Dong J, Shirakawa A, Ueda K I and Kaminskii A A 2007 *Appl. Phys.* B **89** 359–65
[30] Dong J, Shirakawa A, Ueda K I and Kaminskii A A 2007 *Appl. Phys.* B **89** 367–76
[31] Millar P, Birch R B, Kemp A J and Burns D 2008 *IEEE J. Quantum Electron.* **44** 709–17